Journal Name RSCPublishing

ARTICLE

Cite this: DOI: 10.1039/x0xx00000x

Received 00th January 2012, Accepted 00th January 2012

DOI: 10.1039/x0xx00000x

www.rsc.org/

New diclofenac salts with the dense hydrogen bond donor propane-1,3-diaminium

Jaxon R. Breckell, Luke Conte, Michael W. Potts, Pradnya S. Sawant, Raymond J. Butcher, Beena K. Vernekar, and Christopher Richardson

A series of solvatomorphic structures of the anti-inflammatory drug diclofenac (dcfn⁻) and the dense hydrogen bond donor propane-1,3-diaminium (H₂pn²⁺) are reported. Single crystal X-ray diffraction shows each structure contains a dcfn2·H2pn formula unit (1) with solvent of crystallisation [1·2H₂O, 1·3H₂O, 1·2MeOH, 1·EtOH·2H₂O, 1·PrOH, 1.2DMSO]. The propane-1,3-diaminium molecules evoke extensive networks of hydrogen-bonded interactions with the solvates and the dcfn carboxylate groups. All structures are lamellar with hydrophilic solvate-containing sheets separating hydrophobic layers of aromatic dcfn moieties. Supporting characterisations by powder X-ray diffraction, Fourier transform infrared and ¹H NMR spectroscopies, thermal analysis (TG-DSC) and elemental microanalysis were used to reveal the sometimes delicate phase distributions amongst this set of compounds. TG-DSC showed a consistent pattern across the water and alcohol-containing compounds with desolvation occurring before melting to an anhydrous ionic liquid form around 140-150 °C. Heating to approximately 200 °C induces a minor dehydration reaction that covalently links diclofenac and propan-1,3diaminium molecules via amide bond formation. A mechanochemical synthetic route to 1.3H₂O was determined and this compound was selected for study by gravimetric water vapour adsorption. These studies showed the lamellar structure of 1.3H₂O displays reversible but imperfect water adsorption between 0% and 50% relative humidity, which is ascribed to some crystal fatigue. This work expands crystal engineering strategies for new and existing active pharmaceutical ingredients to low molecular weight diamines.

Introduction

Diclofenac acid (Hdcfn) is a potent nonsteroidal antiinflammatory drug (NSAID) of the phenylalkanoic acids group and is used therapeutically in inflammatory, analgesic and antipyretic treatments. ¹⁻³ In addition, the use of NSAIDs has become documented as an adjunct therapy for COVID-19 patients in recent times. ⁴ The poor solubility ⁵ and gastrointestinal side effects of Hdcfn are well-documented and alternative formulations and derivatives to enhance efficacy are popular targets to improve this drug.

Strategies to improve the delivery of dcfn are the preparation of coordination compounds⁶⁻¹² and of multicomponent solids, such as co-crystals and organic salts.^{13, 14} Pyridine-based molecules have proved popular for co-crystallisation with dcfn,¹⁵ particularly for crystal engineering supramolecular structures.¹⁶ There are a number of organic salts of diclofenac (see Table S1 for a selection) of which the vast majority are 1:1 salts with protonated amines. One of the most notable is the diethylammonium

salt,¹⁷ which is the active ingredient found in the topical formulation of Voltaren® emulgel. It is also notable that there are very few salts featuring multi-cationic ammonio molecules crystallised with dcfn. However, this could be a strategy for obtaining higher drug loading. For example, Lynch and co-workers reported the 3:1 organic salt of dcfn with triprotonated tris(2-ethylamine)amine.¹⁸ Here, we present several new solvatomorphic 2:1 salts of dcfn and propane-1,3-diaminium (Fig. 1) and the investigation of their structures and selected properties. Propane-1,3-diaminium cations are perhaps underutilised as counterions for active pharmaceutical ingredients but, nevertheless, were shown to have beneficial effects for dissolution and oral bioavailability for the antihypertensive drug Candesartan.¹⁹

Fig. 1 The structures of diclofenac and propane-1,3-diaminium.

Experimental

All chemicals used were of analytical grade and purchased from either Sigma Aldrich, VWR Australia or Ajax Finechem Pty Ltd. All alcohols were dried over sequential batches of activated 3 Å sieves before use. ¹H NMR and ¹³C NMR spectra were obtained using a Bruker NMR spectrometer operating at 400 MHz for ¹H and 101 MHz for ¹³C. ¹H NMR spectra were referenced to the residual protio peaks at 2.50 ppm (DMSO-*d*₆) or 7.27 ppm (CDCl₃). ¹³C NMR spectra were referenced to the solvent peaks at 39.6 ppm (DMSO-*d*₆) or 77.7 ppm (CDCl₃). Fourier transform infrared (FTIR) spectra were recorded in ATR mode using a Bruker Vertex 70 FTIR spectrometer between 400 cm⁻¹ – 4000 cm⁻¹ and processed using OPUS software (Version 7.8).

Simultaneous thermogravimetric and differential scanning calorimetry (TG-DSC) data were recorded using a Netzsch STA449F3 SiC furnace at 10 °C·min under N2 flow at 20 cm³·min and 10 °C·min¹ under 5% O2 in N2 flow at 40 cm³·min⁻¹. TG-DSC data for water vapour isotherms were collected under isothermal conditions of 40 °C using a Cu furnace equipped with a modular humidity generator attachment (ProUmid GmbH & Co. KG, MHG32) and mixer module with an external, adjustable temperature zone controller. The humidity was controlled via a programmed experiment on MHG32 software, and in a humidified nitrogen gas flow of 150 cm³·min⁻¹. Samples of approximately 5–6 mg were placed into concavus aluminium pans without lids for these measurements.

Powder X-ray diffraction (PXRD) patterns were recorded in reflection mode on a PANalytical Aeris X-ray diffractometer with Cu K α radiation (λ = 1.5405980; 40 kV, 15 mA) equipped with a PIXcel1D-Medipix3 detector. Experimental settings in the 2 θ angle range of 3–40° with 0.02° step size were used.

Single crystal X-ray diffraction (SCXRD) data were collected using a XtaLAB Mini II diffractometer with Mo K α radiation (λ = 0.71073 Å) and a HyPix HPC detector or a XtaLAB Synergy diffractometer with Cu K α (λ = 1.54184) radiation. The data were integrated and scaled with CrysAlisPro 1.171.41.123a (Rigaku Oxford Diffraction, 2022) with empirical absorption correction using spherical harmonics, as implemented in SCALE3 ABSPACK scaling algorithm. The crystal structures were solved by direct methods using SHELXT²⁰ and refined against F² on all data

by full-matrix least-squares with SHELXL²¹ under Olex2.²² Hydrogen atoms on the water molecules in 1·3H₂O were refined subject to distance restraints. Hydrogen atoms on the propane-1,3-diaminum cations, the alcohol molecules and the carbons of dcfn anions were placed in calculated positions and in appropriate riding models in all the structures.

Mechanochemical synthesis was carried out using the Domel Mix-Mill 20 in 10 mL stainless steel jars with a single stainless steel ball bearing of 7 mm diameter at a frequency of 18 Hertz.

Elemental microanalysis was performed by the Chemical Analysis Facility, Macquarie University, Australia.

Synthetic procedure for 1.3H₂O

A solution of cobalt acetate tetrahydrate (249 mg, 1.0 mmol) in methanol (10 mL) was added to a solution of acetylacetone (0.102 mL, 1.0 mmol) and diaminopropane (0.083 mL, 1 mmol) in methanol (10 mL). The contents were stirred for two hours at room temperature. A solution of sodium diclofenac (318 mg, 1 mmol) in methanol (15 mL) was added. The pH of the solution was around 8. Stirring was continued for three hours and then the solution was stored for crystallization. After a few weeks some fawn-coloured crystals formed and were harvested by filtration. No yield was recorded. Found: C, 51.65%; H, 5.39%; 9.22%; N, Calc. for (C₁₄H₁₀Cl₂NO₂)₂·C₃H₁₂N₂·3H₂O: C, 51.68%; H, 5.32%; N, 7.78%.

Direct solution phase synthesis of 1.3H2O

An aqueous solution (1 mL) containing 1,3-diaminopropane (10.0 μ L, 0.112 mmol) and trifluoroacetic acid (15.5 μ L, 0.201 mmol) was added in one portion to a rapidly stirred solution of Nadcfn (63.8 mg, 0.200 mmol) dissolved in water (4 mL). An immediate white precipitate developed. The mixture was stirred for a few minutes before the solid was collected by filtration and washed with water (3 × 0.5 mL) and air dried overnight. Yield 53.3 mg (74%); Found C, 51.74%; H, 5.28%; N, 7.64%; Calc. for (C₁₄H₁₀Cl₂NO₂)₂·C₃H₁₂N₂·(H₂O)₃: C, 51.68%; H, 5.32%; N, 7.78%.

Mechanosynthesis of 1.3H2O

Hdcfn (59.7 mg, 0.202 mmol), 1,3-diaminopropane (8.5 μ L, 0.10 mmol), H₂O (5.5 μ L, 0.31 mmol) and ethanol or isopropanol (15.0 μ L, 0.26 mmol) were placed into a 5 mL stainless steel milling jar and milled at 18 Hz for 30 mins with a single steel ball bearing. The milling jar was opened to inspect the contents at this time and any material on the sides was scraped down. The jar was resealed, and milling resumed for another 90 mins at 18 Hz, giving a free-flowing powder. The compound was dried under vacuum at room temperature. The recovered yields were near-quantitative. ¹H NMR analysis showed no incorporation of any alcohol.

Synthesis of 1·2MeOH

1,3-Diaminopropane (22.0 μ L, 0.261 mmol) was added to Hdcfn (119.9 mg, 0.405 mmol) dissolved in warm dry methanol (2.0 mL) under constant stirring. The solution was

left to stand at room temperature in a capped vial. After 5 days, the crystals that had formed were harvested by filtration and sparingly washed with cold dry methanol (2 \times 0.5 mL) and diethyl ether (2 \times 0.5 mL). Yield: 72.7 mg (50%). Found C, 54.28%; H, 5.80%; N, 7.64%; Calc. for (C₁₄H₁₀Cl₂NO₂)₂·C₃H₁₂N₂·2CH₃OH: C, 54.26%; H, 5.52%; N, 7.67%.

Reaction in reagent grade MeOH

1,3-Diaminopropane (22.0 μ L, 0.261 mmol) was added to Hdcfn acid (119.8 mg, 0.404 mmol) dissolved in warm reagent grade methanol (2.0 mL). The solution was swirled and left to stand at room temperature in a capped vial. Crystals formed over 24 hours and were harvested by filtration after 5 days and washed sparingly with a small volume of cold methanol then diethyl ether and air dried. Yield 67.7 mg (~47%).

Reaction in MeOH-H₂O

Hot water (2.0 mL) was added to a solution of Hdcfn (59.2 mg, 0.200 mmol) and 1,3-diaminopropane (10.0 μ L, 0.112 mmol) in warm methanol (2.0 mL). The resulting solution was swirled, capped, and left to stand at room temperature. Crystals had formed after 1 hour and were harvested by filtration the next day and washed sparingly with cold 1:1 methanol-water (2 × 0.5 mL) and then methanol (1 × 0.25 mL) and air dried. Yield 44.8 mg.

Synthesis of 1·EtOH·2H₂O

Reaction in dry EtOH

This synthesis was carried out as described above for the reaction in methanol solution with the following quantities: Hdcfn (59.7 mg, 0.202 mmol), 1,3-diaminopropane (10.0 μ L, 0.112 mmol), EtOH (2.0 mL). Washed with chilled EtOH (2 × 0.5 mL) and diethyl ether (2 × 0.5 mL). Yield 48.8 mg (65%). Found C, 54.51%; H, 5.41%; N, 7.61%; Calc. for (C₁₄H₁₀Cl₂NO₂)₂·C₃H₁₂N₂·EtOH·H₂O*: C, 54.26%; H, 5.52%; N, 7.67%. * Sample loses H₂O.

Reaction in reagent grade EtOH

This synthesis was carried out as described above for the reaction in methanol solution with the following quantities: Hdcfn (59.7 mg, 0.202 mmol), 1,3-diaminopropane (10.0 μ L, 0.112 mmol), EtOH (2.0 mL). Washed with EtOH (2 × 0.5 mL) and diethyl ether (4 × 0.5 mL). Yield 49.9 mg.

Reaction in EtOH-H₂O

This synthesis was carried out as described above for the reaction in methanol-water solution with the following quantities: Hdcfn (59.3 mg, 0.205 mmol), 1,3-diaminopropane (10.0 μ L, 0.112 mmol), EtOH (2.0 mL), H₂O (2.0 mL). Crystals were collected by filtration after approximately half the solution had evaporated and were washed with EtOH (2 × 0.5 mL) and diethyl ether (2 × 0.5 mL). Yield 44.7 mg. Found C, 52.73%; H, 5.50%; N, 7.88%; Calc. for (C₁₄H₁₀Cl₂NO₂)₂·C₃H₁₂N₂·½EtOH·2H₂O: C, 52.98%; H, 5.42 %; N, 7.72%.

Reaction in dry ⁱPrOH

This synthesis was carried out as described above for the reaction in methanol solution with the following quantities: Hdcfn (61.7 mg, 0.205 mmol), 1,3-diaminopropane (10.0

 μ L, 0.112 mmol), PrOH (2.0 mL). Washed with PrOH (2 × 0.5 mL) and diethyl ether (2 × 0.5 mL). Yield 63.0 mg; Found C, 53.30%; H, 5.42%; N, 7.49%; Calc. for (C₁₄H₁₀Cl₂NO₂)₂·C₃H₁₂N₂·½PrOH·2H₂O: C, 53.29%; H, 5.50%; N, 7.65%.

Synthesis of 1.2H2O in PrOH-H2O

This synthesis was carried out as described above for the reaction in methanol-water solution with the following quantities: Hdcfn (59.3 mg, 0.205 mmol), 1,3-diaminopropane (10.0 μ L, 0.112 mmol), 4 PrOH (2.0 mL), H₂O (2.0 mL). Crystals were collected by filtration after approximately half the solution had evaporated and washed with 4 PrOH (2 × 0.5 mL) and diethyl ether (2 × 0.5 mL). Yield 51.6 mg (72%); Found C, 53.07%; H, 5.33%; N, 7.55%; Calc. for (C₁₄H₁₀Cl₂NO₂)₂·C₃H₁₂N₂·2H₂O: C, 53.00%; H, 5.17%; N, 7.98%.

Reaction in *n*-Propanol

1,3-Diaminopropane (10.0 μ L, 0.122 mmol) was added to Hdcfn (61.8 mg, 0.209 mmol) dissolved in dry "PrOH (7 mL) under constant stirring. The solution was left to stand at room temperature in an uncapped vial. Crystals formed over 24 hours and were collected by vacuum filtration after 24 hours. The crystals were washed with cold "PrOH (2 \times 2 mL) then diethyl ether (2 \times 0.5 mL) and air dried. Yield: 50.7 mg. Found C, 54.62%; H, 5.28%; N, 7.98%; Calc. for (C₁₄H₁₀Cl₂NO₂)₂·C₃H₁₂N₂·½"PrOH·H₂O: C, 54.63%; H, 5.36%; N, 7.84%.

Synthesis of 1.2H2O in "PrOH-H2O

This synthesis was carried out as described above for the reaction in methanol-water solution with the following quantities: Hdcfn (59.7 mg, 0.202 mmol), 1,3-diaminopropane (10.0 μL , 0.112 mmol), "PrOH (2.0 mL), H2O (2.0 mL). Crystals were collected by filtration after approximately half the solution had evaporated and were washed with cold "PrOH (2 × 0.5 mL) and diethyl ether (2 × 0.5 mL). Yield 44.6 mg (64%). These crystals were found to be the dihydrate form $1\cdot 2 H_2 O$ from diffraction studies and $^1 H$ NMR analysis.

Reaction in "BuOH

This synthesis was carried out as described above for the reaction in methanol with the following quantities: Hdcfn (61.4 mg, 0.207 mmol), 1,3-diaminopropane (10.0 μ L, 0.122 mmol), "BuOH (2 mL). Washed with cold "BuOH (2 × 1 mL) and diethyl ether (2 × 0.5 mL) and air dried. Yield: 46.1 mg. Found C, 55.66%; H, 5.28%; N, 8.14%; Calc. for (C₁₄H₁₀Cl₂NO₂)₂·C₃H₁₂N₂·½"BuOH·½H₂O: C, 55.47%; H, 5.23%; N, 8.00%.

Reaction in 'BuOH

This synthesis was carried out as described above for the reaction in methanol solution with the following quantities: Hdcfn (59.7 mg, 0.202 mg), 1,3-diaminopropane (10.0 μ L, 0.112 mmol), 'BuOH (2.0 mL). Washed with dry 'BuOH (2 \times 0.5 mL) and diethyl ether (2 \times 0.5 mL). Yield 37.2 mg. Found C, 53.67%; H, 5.33%; N, 7.63%; Calc. for (C₁₄H₁₀Cl₂NO₂)₂·C₃H₁₂N₂·½'BuOH·1.66H₂O: C, 53.85%; H, 5.40%; N, 7.77%.

Synthesis of 1.2H₂O in ^tBuOH-H₂O

This synthesis was carried out as described above for the reaction in methanol-water solution with the following quantities: Hdcfn (59.3 mg, 0.201 mmol), 1,3-diaminopropane (10.0 $\mu L,$ 0.112 mmol), 'BuOH (2.0 mL), H2O (2.0 mL). Crystals were collected by filtration after approximately half the solution had evaporated and washed with 'BuOH (2 \times 0.5 mL) and ethyl acetate (2 \times 0.5 mL). Yield 51.8 mg (72%); These crystals were found to be the dihydrate form $1\cdot 2 \rm{H}_2 \rm{O}$ from diffraction studies and $^1 \rm{H}$ NMR analysis.

Data for 1.2DMSO

Found C, 51.07%; H, 5.33%; N, 6.81%; Calc. for $(C_{14}H_{10}Cl_2NO_2)_2\cdot C_3H_{12}N_2\cdot 2(C_2H_6SO)$: C, 51.10%; H, 5.39%; N, 6.81%.

Results and discussion

Fawn-coloured crystals were isolated after several weeks from a reaction of Co(OAc)2·4H2O, acetylacetone, propane-1,3-diamine and sodium diclofenac in methanol at room temperature. SCXRD analysis showed the structure crystallises in the triclinic space group P-1 with two dcfn anions, one propane-1,3-diaminium dication and three water molecules in the asymmetric unit (Fig. 2), to give the formula (dcfn)₂(H₂pn)·3H₂O (1·3H₂O). The dcfn anions display near-identical conformations (Fig. S15) with the characteristic intramolecular hydrogen bond between aryl amine NH and carboxylate groups (N···OCO, 2.877(1) Å and 2.872(1) Å). The dcfn anions pack remarkably efficiently without obvious strong and distinctive interactions. There are rather long C-H \cdots π interactions between one of the methylene protons and adjacent phenylacetic acid rings (unique distances 2.891(2) and 2.958(2) Å) leading to 'slip-stacking' in the b-axis direction. The anions self-assemble into hydrophobic layers in the structure with their outwardly-facing carboxylate groups engaging in a complex pattern of hydrogen-bonding with the water molecules and propane-1,3-diaminium cations. The diaminium cations lie approximately parallel to the a-axis in an anti-gauche conformation with the amine group N5S rotated away from co-linearity with the rest of the molecule. The cations are compact hydrogen bond donors and are the foci for organising the water molecules and carboxylate groups of dcfn anions (Fig. 3). All NH bonds are utilised to bind four water molecules and three dcfn anions and there are two longer C-H contacts to O2B and O1A# (2.35 Å and 2.51 Å, respectively). Thus, the diaminium cations are high density H-bond donors. Table S3 presents the donoracceptor distances for these interactions, which all fall within expected values. The multiple H-bonding environments are manifest in the FTIR spectrum of 1.3H2O as a large broad band from 3700-2200 cm⁻¹ (Fig. S1). This feature was observed in the spectra of all the salts analysed by FTIR in this work and indeed the spectra are highly similar.

The extensive hydrogen-bonding involving the diaminium cations, water molecules and defn carboxylate anions perpetuates in the *ab*-plane. The supramolecular structure is organised into alternating hydrophobic-hydrophilic layers that stack in the *c*-axis direction, as shown in Fig. 4. 1·3H₂O shares its structural features with a piperizinium diclofenac structure, (dcfn)₂H₂pz·2H₂O,²³ which is also organised via a network of charge-assisted H bonds into alternating hydrophilic-hydrophobic layers, suggesting this kind of structure may be reliably formed with small diamines.

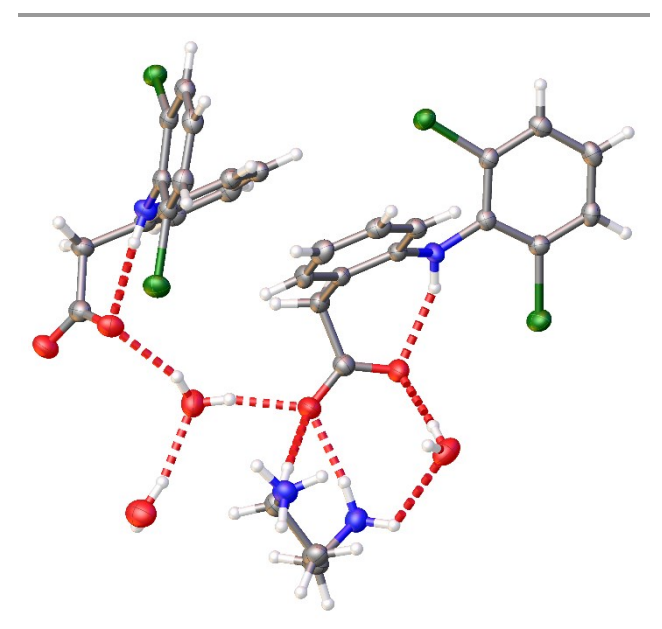


Fig. 2 A perspective view of the asymmetric unit in $1\cdot3H_2O$. Hydrogen bonding interactions are displayed as red dashed lines. ADPs are displayed at the 50% probability level.

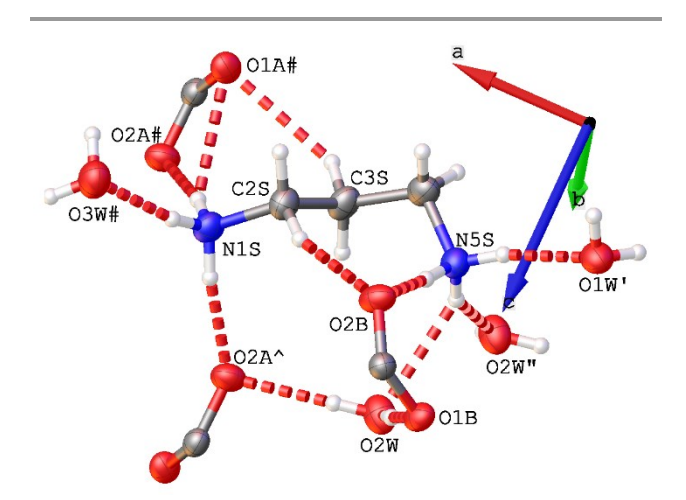


Fig. 3 H-Bond donor contacts from propane-1,3-diaminium cations in the structure of $1\cdot3H_2O$. Hydrogen bonding interactions are displayed as red dashed lines. ADPs are displayed at the 50% probability level. Symmetry codes: '= 1-X,1-Y,1-Z; "= 1-X,2-Y,1-Z; "= 1-X,1-Y,1-Z; "= 1-X,1-

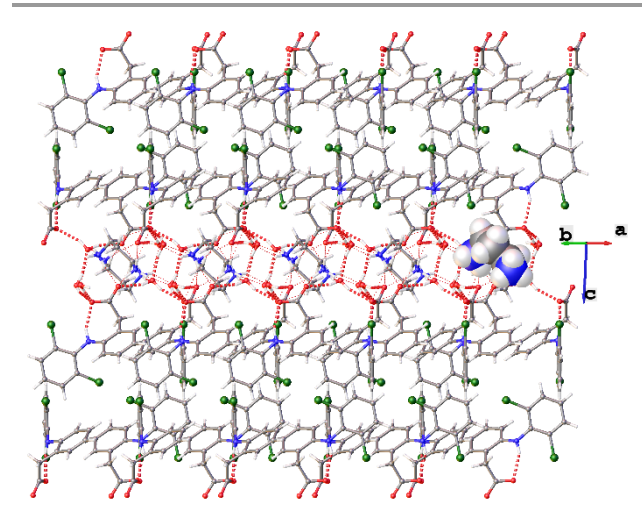


Fig. 4 A view in the [110] direction in $1 \cdot 3H_2O$ showing the carboxylate groups of the dcfn anions directed to the outsides of the hydrophobic layers. One molecule of propane-1,3-diaminium is shown in space filling form to accentuate its orientation in the hydrophilic layers.

Direct Hydrothermal and Mechanochemical Syntheses of $1.3H_2O$

Microcrystalline 1·3H₂O formed in good yield when propane-1,3-diaminium bistrifluoroacetate was added to two equivalents of sodium diclofenac dissolved in water. Characterisation by FTIR (Fig. S1), PXRD (Fig. S28), TG-DSC (Fig. S37) and microanalysis confirmed phase purity of this compound.

Mechanochemical methods offer new vistas for chemical synthesis, ²⁴⁻²⁶ particularly for cocrystals and organic salts, ²⁷, ²⁸ and efficient low-solvent synthetic routes to small sized particles. PXRD analysis showed that 1.3H2O did not form from a mechanochemical synthesis of Hdcfn, propane-1,3diamine and water in the 2:1:3 molar ratio, respectively, that reflects its stoichiometry. Liquid assisted grinding (LAG) extends traditional mechanochemistry by employing small amounts of solvent to enhance reactivity. 26 In our case, using ethanol or isopropanol as a LAG solvent (approximately equimolar with H2O) gave a tremendous improvement and 1.3H₂O was formed quantitatively and phase pure after 2 hours of milling at 18 Hz (Fig. S29). Key to the successful mechanosynthesis was the low milling frequency and progress toward completion of the reaction was assessed at time points by PXRD. Interestingly, the mechanochemical method showed the trihydrate form was much preferred over the ethanol or isopropanol solvates that crystallise from solution (vide infra).

Crystals were observed to form in the DMSO-*d*6 solutions used for ¹H NMR spectroscopic analysis of the products from mechanochemical syntheses. Therefore, 1·3H₂O was dissolved in hot DMSO to yield crystals suitable for SCXRD. The structural analysis showed this was a new crystal form with one dcfn anion, half a propane-1,3-diaminium dication and one disordered DMSO solvate

crystallised in the asymmetric unit of the space group *Pccn* (Fig. S16), resulting in a formula of (dcfn)₂(H₂pn)·2DMSO (1.2DMSO) (Fig. S17). Bulk purity of this compound was established through microanalysis. 1.2DMSO shares structural features with 1.3H2O. The dcfn anions again pack back-to-back in hydrophobic layers with their carboxylate groups making charge-assisted hydrogen bonds to propane-1,3-diaminium cations, which, in turn, hydrogen bond to the disordered DMSO molecules. The cations are again dense Hbond donors, using all NH bonds to organise four dcfn anions and two DMSO molecules. The intermolecular contacts are the same at each N terminus of the diaminium cations by virtue of its location across a crystallographic 2-fold axis (Fig. 5), which dictates an anti-anti conformation. The supramolecular structure is arranged in a similar lamellar fashion to 1.3H2O with dcfn layers separated by H2pn-DMSO layers, this time in the ac-plane (Fig. 6). The separation between hydrophobic dcfn layers is greater in 1.2DMSO (~8 Å) than in $1.3H_2O$ (~4 Å) because the diaminium cations lie approximately perpendicular to the dcfn layers in 1.2DMSO (Fig. 6), rather than approximately parallel in 1.3H₂O (Fig. 4).

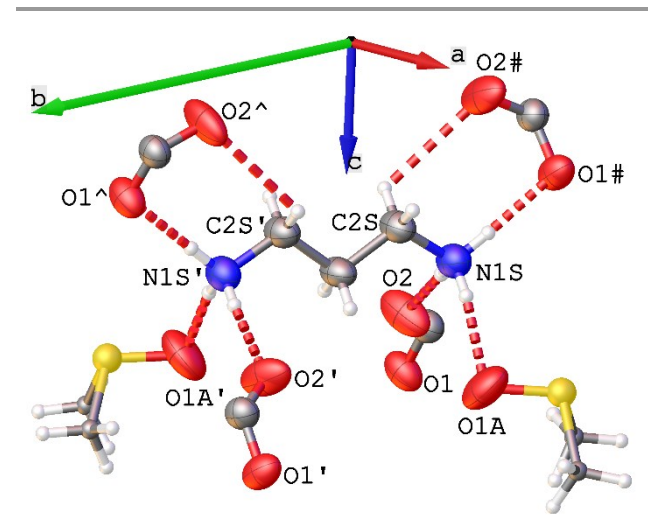


Fig. 5 H-Bond donor contacts from propane-1,3-diaminium cations in the structure of $1\cdot2$ DMSO. Hydrogen bonding interactions are displayed as red dashed lines. ADPs are displayed at the 50% probability level. Carbon and sulfur atoms of DMSO molecules are shown as small spheres for clarity. Symmetry codes: ' = 3/2-X, 3/2-Y, +Z; ^ = +X, 3/2-Y, -1/2+Z; # = 3/2-X, +Y, -1/2+Z

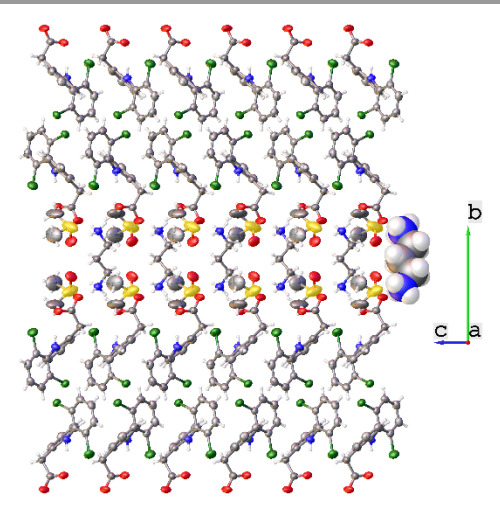


Fig. 6 A view in the [100] direction of **1**·2DMSO showing the spacing between hydrophobic layers due to the orientation of the propane-**1**,3-diaminium cations. One molecule of propane-**1**,3-diamidinium is shown in space filling form to accentuate its orientation. Only one position of the disordered DMSO molecules is shown for clarity.

Crystal Engineering Alcohol Solvates

We anticipated the Hdcfn and propane-1,3-diamine system may be amenable to crystal engineering solvates with low molecular weight alcohols. Indeed, Diclofenac has been found to form a range of solvates with Berberine²⁹ and Clofaziminium.³⁰ We therefore carried out reactions maintaining the 2:1 ratio of dcfn:propane-1,3-diamine under low water conditions (no added water) and high water conditions (equivolume alcohol-water mixtures) in methanol, ethanol, isopropanol, *n*-propanol, *n*-butanol and *tert*-butanol.

Methanol

SCXRD analysis revealed that crystallisation from dry methanol solution yielded crystals in the triclinic space group *P*-1 with the formula (dcfn)₂(H₂pn)·2MeOH (1·2MeOH) (Fig. S18). The diaminium cations are disordered, with the major component (0.89) having an *antianti* conformation and the minor component existing in an *anti-gauche* conformation. The H₂pn cations utilise all N-H donor bonds to organise five dcfn anions and a methanol molecule (Fig. 7).

The supramolecular crystal structure is near identical to the hydrophobic-hydrophilic lamellar structure of $1\cdot3H_2O$. The layers of H_2 pn cations and methanol solvates perpetuate in the *ab*-plane, separated by dcfn anions in the *c*-direction. 1H NMR spectroscopy (Fig. S2) and microanalytical data supported $1\cdot2$ MeOH as the sole phase. The proportion of $1\cdot2$ MeOH drops to approximately 83% when reagent grade MeOH is used (Fig. S3) with the remaining being $1\cdot3H_2O$, as found by SCXRD cell determinations. Interestingly, SCXRD analyses identified that the first crystals to form in these reactions with reagent grade solvent are, in fact, $1\cdot3H_2O$. We proffer this phase forms and depletes water in the solution aiding crystallisation of $1\cdot2$ MeOH.

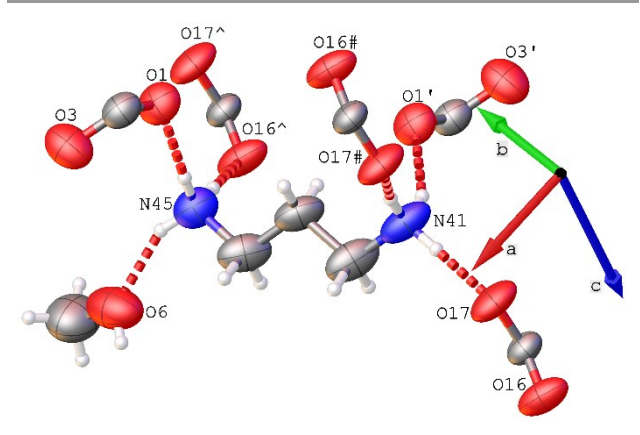


Fig. 7 H-Bond contacts from propane-1,3-diaminium cations in the structure of $1\cdot2$ MeOH. Hydrogen bonding interactions are displayed as red dashed lines. Only the major component of the disordered cation is shown (0.89), for clarity. ADPs are displayed at the 50% probability level. Symmetry codes: ' = $1\cdot X$, $1\cdot Y$, $1\cdot Z$; ' = +X, 1+Y, +Z; # = $1\cdot X$, -Y, $1\cdot Z$.

Crystallisation under the equivolume methanol-water conditions reversed the phase distribution, with 1.3H2O being the dominant phase and approximately 28% being 1.2MeOH (Fig. S4). These results indicate a competitive balance between the 1.3H2O and 1.2MeOH phases in the methanol-water solvent system. We carried out many single SCXRD cell determinations from crystallisations and did not observe any evidence for a phase contained MeOH and water, for $1 \cdot \text{MeOH} \cdot 2\text{H}_2\text{O}$.

Ethanol

Crystals started forming after a few minutes after adding propane-1,3-diamine to Hdcfn in ethanol solutions. Crystallisation under the ethanol-water conditions took several days and occurred after some solvent evaporation. In both cases, ¹H NMR spectroscopic and microanalytical data were used in combination to afford compositions for the bulk solids. The product that was obtained from dry EtOH analysed as 1·EtOH·2H₂O from ¹H NMR spectroscopy (Fig. S5). When the reaction was carried out in reagent grade EtOH the solid analysed as 1.5%EtOH.2H2O in ¹H NMR spectra (Fig. S6) and TG-DSC. Under the equivolume EtOHwater condition the bulk solid analysed as 1.1/2EtOH.2H2O from ¹H NMR (Fig. S7), TG-DSC (Fig. S42) and elemental microanalysis. This is consistent with the results obtained from MeOH solutions, where the water content in the solvent controls the phase distribution.

SCXRD cell determinations revealed that the first crystals to form in the reagent grade EtOH and equivolume conditions were 1·3H₂O, and that each synthesis also gave a new crystal form with identical triclinic cell dimensions. Full diffraction analysis determined a formula of 1·EtOH·2H₂O for the new form; the asymmetric unit in the space group *P*-1 contained two dcfn anions, one disordered propane-1,3-diaminium dication, one ethanol molecule disordered over three positions and two well-ordered water molecules (Fig. S19). The dcfn anions have essentially identical geometries

(Fig. S20) while the disordered H₂pn cations, which align approximately to the [110] direction, assume *anti-gauche* and *gauche-gauche* conformations for the major (0.57) and minor components, respectively (Fig. 8; Fig. S21).

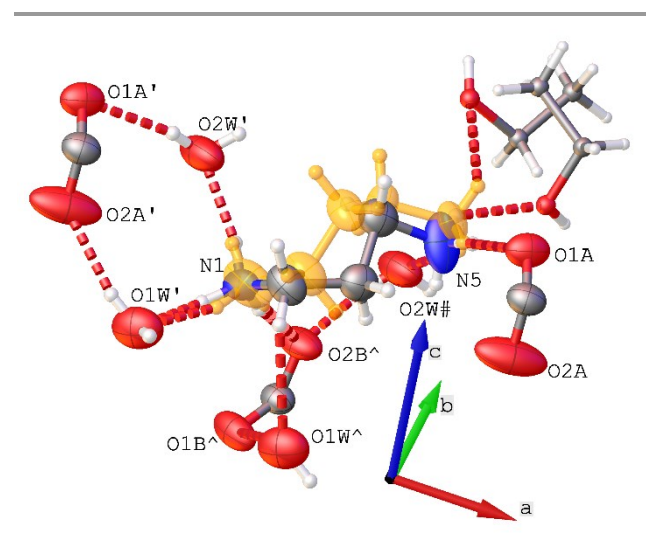


Fig. 8 H-Bond contacts from propane-1,3-diaminium cations in the structure of $1\cdot\text{EtOH}\cdot 2H_2O$. Hydrogen bonding interactions are displayed as red dashed lines. The minor component of the disordered cation is shaded orange (0.43), for clarity. ADPs are displayed at the 50% probability level except for two positions of the disordered EtOH molecules that are displayed as spheres, for clarity. Symmetry codes: '= -1+X, +Y, +Z; $^*= 1-X$, 1-Y, 1-Z; #= -X, 2-Y, 1-Z.

The hydrogen bonding at the N1 terminus of the H₂pn cations is well defined with two water molecules (O1W'; O2W'), which organise linking of dcfn anions along the *a*- and *b*-directions, and a dcfn carboxylate group. The other terminus hydrogen bonds one dcfn carboxylate and the disordered EtOH solvate, which resides in a pocket with multiple hydrogen bonding options available (Fig. S22), thus explaining its disordered nature. The H₂pn cations link the water molecules, which are hydrogen bond donors only to carboxylates, and the dcfn carboxylates into sheets in the *ab*-plane. This structure is also lamellar with the hydrophobic aromatic portions of the dcfn anions stacking in the *c*-direction (Fig. S22).

Isopropanol

A white microcrystalline powder precipitated quickly upon the addition of propane-1,3-diamine to two equivalents of Hdcfn in isopropanol solution and was harvested by filtration. ¹H NMR spectroscopy (Fig. S8) and microanalysis were again used in combination to derive a formula of 1.½¹PrOH·2H2O for the bulk solid. Crystallisation under more dilute conditions (0.05 mM) gave some crystals large enough for SCXRD studies alongside most of the product that appeared poorly crystalline by inspection.

SCXRD showed the asymmetric unit consists of two dcfn anions, one propane-1,3-diaminium dication, and one hydrogen bonded isopropanol solvate molecule (1 PrOH) in the space group *P*-1 (Fig. S23). This result indicates that synthesis under these conditions led to a mixed phase

containing 1^{-1} PrOH as the minor phase amongst other hydrated phases.

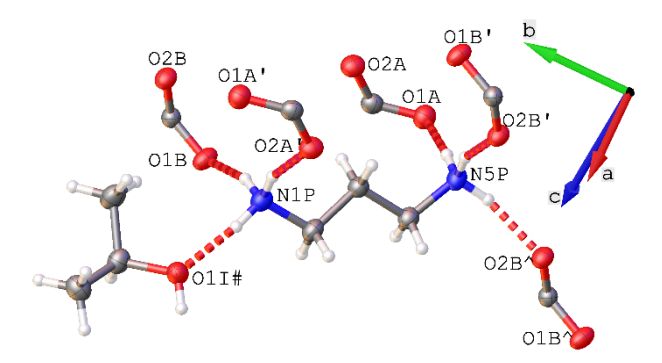


Fig. 9 H-Bond contacts from propane-1,3-diaminium cations in the structure of **1**-'PrOH. Hydrogen bonding interactions are displayed as red dashed lines. ADPs are displayed at the 50% probability level. O1!#···H 1.877(3) Å; O1B····H 1.898(3) Å; O2A'···H 1.862(3) Å; O1A····H 1.818(3) Å; O2B'····H 1.848(3) Å; O2B'····H 1.874(3) Å. Symmetry codes: '= 1-X, 2-Y, -Z; ^= +X, -1+Y, +Z; #= 1+X, +Y, +Z.

The H₂pn molecules have the *anti-anti* conformation and organise three carboxylates at one terminus (N5P) and the alcohol molecule and two more carboxylates at the other (Fig. 9). This is the same result as for $1 \cdot 2$ MeOH; however, the latter compound has room in the lattice for an additional methanol solvate molecule. The dcfn anions have near-identical conformations (Fig. S24) and are linked by H₂pn molecules in the *anti-anti* conformation. The lamellar supramolecular structure of 1^{-i} PrOH shares the same general features as others described here with hydrophilic sheets in the *ab*-plane and stacked in the *c*-direction by the aromatic dcfn anions; this arrangement is shown in Fig. S27.

Crystallisation from the equivolume isopropanol-water conditions gave very large crystals upon evaporation of approximately half the solvent over several days. SCXRD analysis of a cut crystal revealed a new dihydrate phase, 1·2H₂O, in the monoclinic space group P2₁. The asymmetric unit contains four dcfn anions, two propane-1,3-diaminium dications and eight water molecules (Fig. S25). The dcfn anions come in pairs of similar but not identical conformations with the point of difference being the conformation of the carboxylate groups (Fig. S26).

The H₂pn cations lie near-parallel to the *a*-direction and take *anti-anti* and *anti-gauche* conformations (Fig. 10). The *anti-anti* conformer organises two carboxylates and a water at each terminus. This is different to the *anti-gauche* conformer, which organises two carboxylates and a water at one terminus (N5N) and one carboxylate and two water molecules, of which one is disordered (O8WB), at the other. The H-bonding system is propagated into the *ac*-plane by the action of the water molecules and the structure stacks in the *b*-direction with the aromatic dcfn anions, resulting in another lamellar structure. This is shown in Fig. S27 together with similar views for all water and alcohol solvate structures.

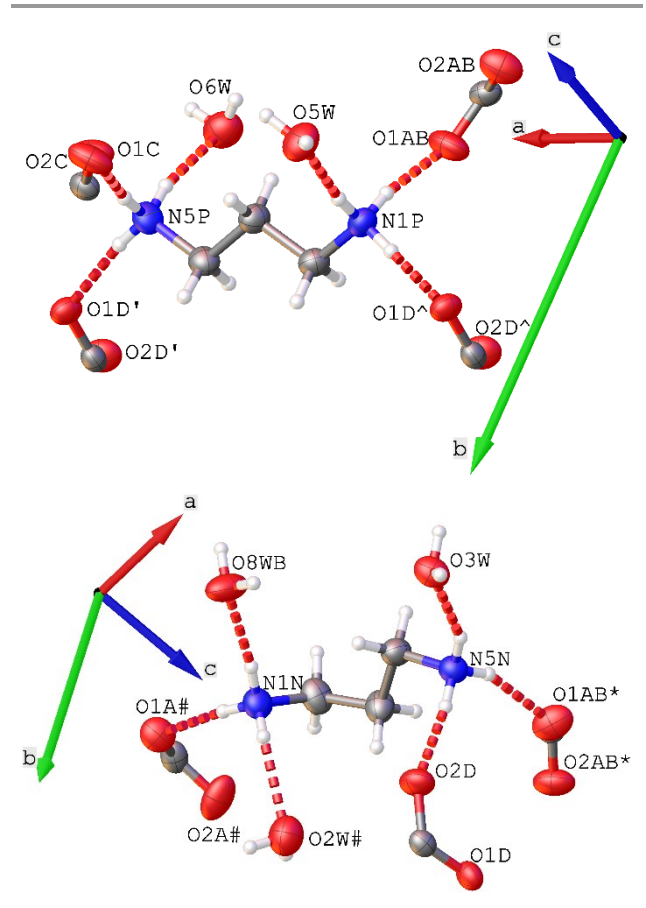


Fig. 10 H-Bond contacts from propane-1,3-diaminium cations in the structure of $1{\cdot}2H_2O$. Shown at top is the *anti-anti* conformer and the *anti-gauche* conformer is shown at the bottom. Hydrogen bonding interactions are displayed as red dashed lines. Only the predominant position of the disordered water molecule is shown (O8WB). ADPs are displayed at the 50% probability level. Symmetry codes: $'=1+X, +Y, -1+Z; ^*=+X, +Y, -1+Z; #=-1+X, +Y, +Z; *=+X, +Y, 1+Z.$

n-Propanol and *n*-Butanol

Reactions in n-propanol and n-butanol quickly led to microcrystalline powders, which were not of sufficient size for SCXRD analysis. The ¹H NMR spectra (Fig. S9-S10) of compounds these showed the 2:1 ratio of diclofenac:propane-1,3-diaminium was maintained and there was half a molecule per formula unit of *n*-propanol and one third of a molecule per formula unit for *n*-butanol. Elemental analyses indicated each compound also crystallised with some water, to give bulk formulas of $1 \cdot \frac{1}{2}$ ⁿPrOH·H₂O and $1 \cdot \frac{1}{3}$ ⁿBuOH· $\frac{1}{2}$ H₂O.

The dihydrate phase, 1·2H₂O, was isolated in good yield after some solvent evaporation in the equivolume *n*-propanol-water conditions. A reaction in *n*-butanol-water was not performed due to only partial miscibility of the solvents.

Tert-butanol

The microcrystalline powder that quickly developed in the reaction solvent of tert-butanol afforded a formula of $1 \cdot \frac{1}{3}$ BuOH for components containing C-H bonds from 1 H NMR spectroscopic analysis. The elemental microanalysis

of the solid was consistent with a formula of $1 \cdot \frac{1}{3}$ BuOH·1.66H₂O. Crystallisation from a more dilute solution, as was done with success for the reaction in isopropanol, did not give the increase in crystallite size needed for single crystal diffraction and further syntheses were not pursued. Crystallisation under the equivolume *tert*-butanol-water conditions gave crystals of $1 \cdot 2$ H₂O in good yield.

Powder X-ray Diffraction Studies

PXRD showed that 1.3H₂O (Fig. S28) and 1.2H₂O (Fig. S30) crystallise in phase-pure form from synthesis in water and the equivolume alcohol-water conditions from isopropanol, *n*-propanol, and *tert*-butanol, respectively. The as-synthesised products from isopropanol, n-propanol, nbutanol and tert-butanol crystallised quickly from these solutions and were mixtures of alcohol and hydrated phases. The experimental PXRD patterns for these compounds are shown in Fig. S31 along with the calculated patterns of 1.1PrOH and 1.2H2O for reference. There is good evidence that the dihydrate phase exists in each of the isolated bulk materials, in line with the microanalytical data. The compound that was analysed by SCXRD from isopropanol, 1. PrOH, is clearly a minor but highly crystalline compound in the mixture from that reaction and the elemental analysis of the bulk mixture indicates a dihydrate phase predominates.

Despite the solvents being dried by standard procedures and stored over activated 3 Å sieves, the bulk samples produced in ethanol, isopropanol, *n*-propanol, *n*-butanol and *tert*-butanol solutions all contain water. We attribute these results to the very high relative humidity in our laboratories (routinely greater than 90% RH) providing sources of water from the atmosphere and glassware in these reactions.

As mentioned previously, 1·2MeOH is produced pure from synthesis in dry methanol solvent and mixed phases containing 1·2MeOH and 1·3H₂O are produced when the solvent contains water, with the ratio between these phases dependent on water content in the reaction solvent. PXRD was less useful for differentiation and phase assignment because of the high similarity in calculated patterns and the experimentally obtained diffraction traces (Fig. S32). The same was true for diffraction analyses from reactions in ethanol and ethanol-water, which showed the same kind of behaviour for the phases 1·EtOH·2H₂O and 1·3H₂O (Fig. S33). Fig. S34 shows the calculated patterns for 1·3H₂O, 1·2H₂O, 1·2MeOH, 1·EtOH·2H₂O, 1·PrOH and 1·2DMSO.

Selective alcohol crystallisation

The structures share considerable similarity, with different alcohol solvates supporting the (dcfn)₂·H₂pn unit. We questioned if there might be selectivity for crystallisation between the alcohols in this system and conducted two further experiments using equal volumes of methanol, ethanol, and the branched alcohols isopropanol and *tert*-butanol in one experiment and methanol, ethanol and the

linear chain alcohols n-propanol and n-butanol in another experiment. Good returns of crystalline solids were obtained from the reactions (Fig. S35-36) and bulk samples were analysed using ¹H NMR spectroscopy in DMSO-d₆ solutions. The spectra showed the 2:1 ratio of dcfn:H2pn was maintained for each experiment and all four alcohols were incorporated in each case. Integration of the signals revealed that methanol, ethanol, isopropanol and tert-butanol were incorporated relative to this formula with 0.43:0.28:0.41:0.04 ratios, respectively (Fig. S12). Thus, methanol and isopropanol are most favoured and crystallisation with tert-butanol is least favoured in this branched system. ¹H NMR integration from the experiment with the linear alcohols revealed a very similar result with methanol and n-propanol being most favoured with a 0.42:0.21:0.27:0.09 ratio of methanol, ethanol, *n*-propanol and *n*-butanol, respectively (Fig. S13), in the bulk solid. These crystals were able to be indexed using SCXRD to a triclinic unit cell typical of the compounds found in this study; however, they also underwent loss of crystallinity and we could not obtain satisfactory diffraction data.

Thermal Analysis

All 'as-synthesised' compounds and 1·2DMSO were analysed by simultaneous thermogravimetric-differential scanning calorimetry (TG-DSC). Fig. 11 shows the thermogravimetrogram for 1·3H₂O recorded under a flowing atmosphere of 10% O₂ in N₂ up to 260 °C (Fig. S37 shows the data up to 600 °C). The endothermic mass loss of 7.5% before 140 °C accounts for the loss of the three waters of crystallisation (calc. 7.5%). The anhydrous compound melts at approximately 150 °C and then undergoes another endothermic mass loss around 200 °C. The further mass loss above this temperature is exothermic and ascribed to decomposition.

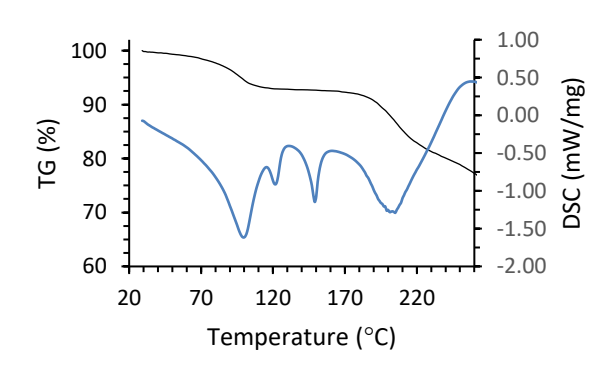


Fig. 11 TG-DSC trace of $1 \cdot 3 \rm{H}_2 \rm{O}$. TG data are shown in black and DSC data in blue.

A sample of the anhydrous compound obtained after heating 1 to its melting point was observed as a shiny liquid (Fig. S38). Further TG-DSC experiments established this did not crystallise upon cooling or melt upon re-heating and, therefore, is an ionic liquid containing diclofenac and was

denoted as **1-IL**. Recently, an imidazolium-diclofenac ionic liquid was reported.³¹ **1-IL** did not transform into **1**·3H₂O or **1**·2H₂O after more than three weeks of atmospheric exposure and further TG-DSC analysis showed it maintained its anhydrous composition (Fig. S39).

The TG-DSC trace of 1.2MeOH shows a higher onset temperature and a more abrupt mass loss for the solvate methanol (calc. 8.8%; found 8.6%) compared to water (Fig. S40). This was true for the mixed phases that result from reactions in ethanol, isopropanol, n-propanol, n-butanol and tert-butanol, likely indicating stronger bonding to the alcohols (Fig. S41-46). The TG-DSC data for the expected mass losses support the formulations of 1-EtOH-2H₂O, $1 \cdot \frac{1}{2}EtOH \cdot 2H_2O$, $1 \cdot \frac{1}{2}$ PrOH·2H₂O, $1 \cdot \frac{1}{2}^n \text{PrOH} \cdot \frac{1}{2} \text{H}_2 \text{O}$ $1.\frac{1}{2}$ ⁿBuOH· $\frac{1}{2}$ H₂O and $1.\frac{1}{3}$ ^tBuOH·1.66H₂O (Table S4) for the bulk as-synthesised solids. All dehydrated or desolvated compounds have similar melting points around 150 °C and have the endothermic event around 200 °C. The compound 1.2DMSO, in contrast, does not lose solvent before melting at 127 °C. After this point, solvent volatilisation and the endothermic reaction appear to co-occur, with the peak in the DSC for these processes at 199 °C (Fig. S47).

The endothermic event at approximately 200 °C in all these samples piqued our curiosity. Bulk samples of 1.3H₂O were therefore heated to 200 °C under an N2 atmosphere and held at that temperature for 10 minutes before cooling and analysis using ¹H NMR spectroscopy in DMSO-d₆ solution. The spectrum showed multiple aromatic-containing products are produced. The major product was found to be diclofenac acid, indicating loss of some propane-1,3-diamine, consistent with mass loss observed around this temperature. However, diagnostically, the CH₂ signals for propane-1,3diamine and a defn-containing molecule are maintained in the same relative integrations but in new chemical shifts downfield of their previous position, indicating the formation of a new compound (Fig. S14). The isotopic signature and mass of the base peak at 629 m/z in negative mode ESI mass spectrometry (Fig. S50) led us to identify a minor pathway of amide bond formation between the propane-1,3-diaminium molecules and the carboxylate groups of two dcfn anions with the loss of water (Scheme 1), which is also consistent with the endothermic response with mass loss observed in the TG-DSC measurement.

Scheme 1 The minor dehydration reaction of 1-IL at approximately 200 °C.

Water vapour adsorption studies

We thought the hydrophilic layers in the structure of 1.3H₂O provided ideal pathways for the exit and re-entry of water and that lattice reorganisation might be achievable even in the presence of the strong charge-assisted hydrogen bonds between the propane-1,3-diaminium cations and dcfn carboxylate groups. We therefore studied the performance of 1.3H₂O to changes in relative humidity (RH) using TG-DSC. Fig. 12 shows the results from cycling between 50% RH and 0% RH (see Fig. S48 for all calorific data). The correct mass loss for all three waters is observed on the first desorption cycle (7.5%); however, the incomplete water uptake observed in the first and the second adsorption cycles (6.2%) is indicative of lattice damage during this experiment. The enthalpic change of the first dehydration is 217 kJ/mol (300.9 J/g) which equates to approximately 72 kJ/mol per water molecule. This is similar in value to our findings for water adsorption in reforming charge-assisted hydrogen bonded organic frameworks.^{32, 33}

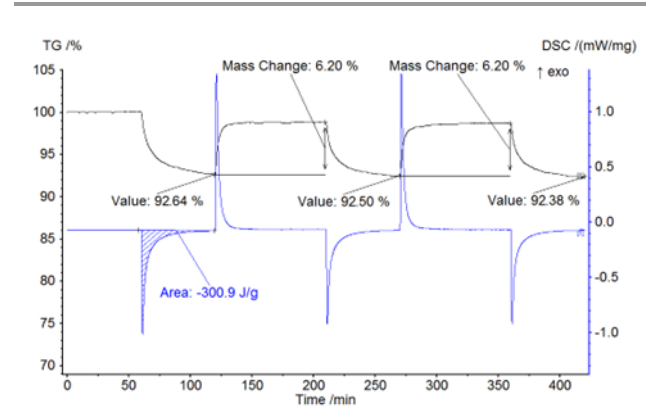


Fig. 12 TG-DSC data of 1.3H $_2$ O for cycling between 50% RH and 0% RH. TG data are shown in black and DSC data in blue.

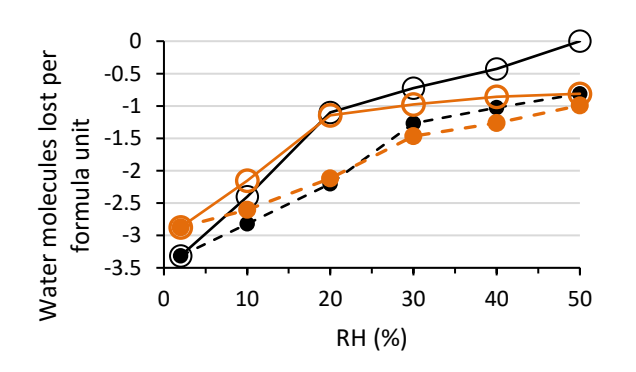


Fig. 13 Water vapour isotherm of $1\cdot 3H_2O$ from a desorption-adsorption-desorption-adsorption sequence. Adsorption points are presented as filled circles connected by dashed lines and desorption points as unfilled circles connected by solid lines. The first desorption-adsorption data are colored in

black, and the second desorption-adsorption data are colored in orange. Lines are provided as a guide for the eye.

To study the water vapour sorption performance in greater detail, we recorded repeated desorption-adsorption cycles in 10% RH increments between 50% and 0% RH. The data are presented as an isotherm in Fig. 13 and as the TG-DSC data with respect to time in Fig. S49. The isotherm shows one water molecule per formula unit is lost between 50% RH and 20% RH on the first desorption leg. Lowering the RH to 10% RH and then to 0% RH results in a mass loss approximately equal to one water molecule per formula unit each time and accounts for the loss of the three waters of crystallisation. However, the first adsorption leg takes up only 2.5 water molecules in total and the performance in the second adsorption and desorption legs is similar.

The mass and calorific data from this experiment clearly show the major desorption change occurs at 10% RH and the major adsorption feature at 20% RH. As was observed in the experiment cycling directly between 50% RH and 0% RH not all water is taken up indicating crystal lattice fatigue or damage at the first cycle. The uptake of 2.5 water molecules is consistent only with incomplete reformation of 1·3H₂O rather than conversion to the dihydrate form, 1·2H₂O.

Conclusions

Lamellar hydrophilic-hydrophobic solids form by the action of the dense H-bond donor, propane-1,3-diaminium, facilitating multiple charge-assisted H-bonds with dcfn anions and further H-bond contacts to solvate molecules in solvatomorphic of series compounds. crystallisations from alcohol-water systems revealed some delicate phase distributions for methanol and ethanol, highlighting the sensitivity of the crystalline product to the reaction conditions. Crystallisations from C3 and C4 alcohol-water mixtures consistently returned the dihydrate structure, on the other hand. Together, these results highlight the robustness of the diaminium cations in structure organisation of dcfn anions and solvates.

The hydrophilic layers in 1·3H₂O provide pathways for the egress and ingress of water to the crystal lattice and our results show water re-uptake is achieved relatively quickly, albeit with some crystal fatigue, in the presence of strong charge-assisted H-bonds between propane-1,3-diaminium cations and anionic dcfn carboxylate groups. The water sorption performance of 1 is an interesting contrast to the anhydrous ionic liquid compound 1-IL, which is formed by melting 1 and is bereft of atmospheric water uptake capabilities. In summary, our work shows small alkyldiamines can be compact, robust and reliable supramolecular synthons and provides new considerations for crystal engineering potentially useful forms for drugs.

Conflicts of interest

There are no conflicts of interest to declare.

Acknowledgements

JRB, LC and MWP acknowledge the Australian Government for Australian Government Research Training Program Awards. CR thanks the University of Wollongong for financial support. BKV acknowledges the Government of Goa and Mr. Prasad Lolayekar, Director, Directorate of Higher Education, Goa, India, for granting sabbatical leave for the year 2022. BKV also thanks Prof. Purnakala Samant, Principal, Government College of Arts, Science and Commerce, Khandola, Goa, for her support.

Notes and references

- ^a School of Chemistry and Molecular Bioscience Science, University of Wollongong, Wollongong NSW 2522, Australia; E-mail: chris_richardson@uow.edu.au
- ^b Department of Chemistry, Government College of Arts, Science and Commerce, Khandola, Marcela, Goa, India; E-mail: beenavernekar@gmail.com
- ^c Department of Chemistry, Howard University, Washington, DC 20059, USA

Electronic Supplementary Information (ESI) available: FTIR spectra, NMR spectra, PXRD data, SCXRD figures and data, additional TG–DSC and mass spectral data. CCDC 2076682 (1·3H₂O), 2210150 (1·2DMSO), 2210151 (1·2MeOH), 2246041 (1·EtOH·2H₂O), 2245277 (1·PrOH), 2245278 (1·2H₂O). These data can be obtained free of charge via www.ccdc.cam.ac.uk/data_request/cif, or by emailing data_request@ccdc.cam.ac.uk, or by contacting The Cambridge Crystallographic Data Centre, 12, Union Road, Cambridge CB2 1EZ, UK; fax: +44 1223 336033.

- B.Chuasuwan, V. Binjesoh, J. E. Polli, H. Zhang, G. L. Amidon, H. E. Junginger, K. K. Midha, V. P. Shah, S. Stavchansky, J. B. Dressman and D. M. Barends, *J. Pharm. Sci.*, 2009, 98, 1206-1219.
- 2. T. G. Kantor, Am. J. Med., 1986, 80, 64-69.
- 3. V. A. Skoutakis, C. A. Carter, T. R. Mickle, V. H. Smith, C. R. Arkin, J. Alissandratos and D. E. Petty, *Drug Intell. Clin. Pharm.*, 1988, **22**, 850-859.
- M. T. Kelleni, Biomed. Pharmacother., 2021, 133, 110982-110985.
- A. Llinàs, J. C. Burley, K. J. Box, R. C. Glen and J. M. Goodman, J. Med. Chem., 2007, 50, 979-983.
- 6. M. Kyropoulou, C. P. Raptopoulou, V. Psycharis and G. Psomas, *Polyhedron*, 2013, **61**, 126-136.
- A. Tarushi, C. P. Raptopoulou, V. Psycharis, C. K. Kontos, D. P. Kessissoglou, A. Scorilas, V. Tangoulis and G. Psomas, *Eur. J. Inorg. Chem.*, 2016, 2016, 219-231.
- G. D. Geromichalos, A. Tarushi, K. Lafazanis, A. A. Pantazaki,
 D. P. Kessissoglou and G. Psomas, *J. Inorg. Biochem.*, 2018, 187,
 41-55.
- C. N. Banti, A. G. Hatzidimitriou, N. Kourkoumelis and S. K. Hadjikakou, *J. Inorg. Biochem.*, 2019, 194, 7-18.

 S. Perontsis, A. Dimitriou, P. Fotiadou, A. G. Hatzidimitriou, A. N. Papadopoulos and G. Psomas, *J. Inorg. Biochem.*, 2019, 196, 110688

- C. Kakoulidou, P. S. Gritzapis, A. G. Hatzidimitriou, K. C. Fylaktakidou and G. Psomas, *J. Inorg. Biochem.*, 2020, 211, 111194
- H. Yasir Khan, S. Parveen, I. Yousuf, S. Tabassum and F. Arjmand, *Coord. Chem. Rev.*, 2022, 453, 214316-214334.
- P. K. Goswami, V. Kumar and A. Ramanan, J. Mol. Struct., 2020, 1210, 128066-112879.
- K. M. O'Connor and O. I. Corrigan, *Int. J. Pharm.*, 2001, 226, 163-179.
- N. B. Báthori, A. Lemmerer, G. A. Venter, S. A. Bourne and M. R. Caira, Cryst. Growth Des., 2010, 11, 75-87.
- Q. Zheng, S. L. Rood, D. K. Unruh and K. M. Hutchins, *Chem. Commun.*, 2019, 55, 7639-7642.
- 17. C. Castellari, F. Comelli and S. Ottani, *Acta Crystallogr. C: Cryst. Struct. Commun.*, 2001, **57**, 437-438.
- 18. D. E. Lynch, A. S. Bening and S. Parsons, *Acta Crystallogr., Sect. E: Struct. Rep. Online*, 2003, **59**, o1314-o1317.
- Y. Chi, W. Xu, Y. Yang, Z. Yang, H. Lv, S. Yang, Z. Lin, J. Li,
 J. Gu, C. L. Hill and C. Hu, *Cryst. Growth Des.*, 2015, 15, 3707-3714.
- 20. G. M. Sheldrick, Acta Cryst., 2015, A71, 3-8.
- 21. G. M. Sheldrick, Acta Cryst., 2015, C71, 3-8.
- O. V. Dolomanov, L. J. Bourhis, R. J. Gildea, J. A. K. Howard and H. Puschmann, *J. Appl. Cryst.*, 2009, 42, 339-341.
- C. Castellari and S. Ottani, Acta Crystallogr. C: Cryst. Struct. Commun., 1998, 54, 415-417.
- S. L. James, C. J. Adams, C. Bolm, D. Braga, P. Collier, T. Friscic,
 F. Grepioni, K. D. Harris, G. Hyett, W. Jones, A. Krebs, J. Mack,
 L. Maini, A. G. Orpen, I. P. Parkin, W. C. Shearouse, J. W. Steed
 and D. C. Waddell, *Chem. Soc. Rev.*, 2012, 41, 413-447.
- J. L. Howard, Q. Cao and D. L. Browne, *Chem. Sci.*, 2018, 9, 3080-3094.
- J. G. Hernández and C. Bolm, J. Org. Chem., 2017, 82, 4007-4019
- T. Friščić, S. L. Childs, S. A. A. Rizvi and W. Jones, CrystEngComm, 2009, 11, 418-426.
- D. Braga, L. Maini and F. Grepioni, Chem. Soc. Rev., 2013, 42, 7638-7648.
- 29. W. Sun, L. Zuo, T. Zhao, Z. Zhu and G. Shan, *Acta Crystallogr. C: Cryst. Struct. Commun.*, 2019, **75**, 1644-1651.
- L. Bodart, M. Prinzo, A. Derlet, N. Tumanov and J. Wouters, CrystEngComm, 2021, 23, 185-201.
- C. C. P. da Silva, B. C. Dayo Owoyemi, B. R. Alvarenga-Jr, N. Alvarez, J. Ellena and R. L. Carneiro, *CrystEngComm*, 2020, 22, 5345-5354.
- S. A. Boer, L. Conte, A. Tarzia, M. T. Huxley, M. G. Gardiner, D.
 R. T. Appadoo, C. Ennis, C. J. Doonan, C. Richardson and N. G.
 White, *Chem. Eur. J.*, 2022, 28, e202201929.
- P. Muang-Non, C. Richardson and N. G. White, *Angew. Chem. Int. Ed.*, 2023, 62, e202212962.